PROCEEDINGS OF SCIENCE

Towards a Laser-driven polarized ^{3}He Ion–Beam Source

Ilhan Engin[*] [a], **Markus Büscher** [b,c], **Oliver Deppert** [d], **Laura Di Lucchio** [e], **Ralf Engels** [a], **Simon Frydrych** [d], **Paul Gibbon** [f], **Annika Kleinschmidt** [d], **Andreas Lehrach** [a,g,h], **Markus Roth** [d], **Friederike Schlüter** [b], **Katharina Strathmann** [b], **Florian Wagner** [d]

[a] *Institut für Kernphysik, Forschungszentrum Jülich GmbH, D-52425 Jülich, DE*
[b] *Peter Grünberg Institut, Forschungszentrum Jülich GmbH, D-52425 Jülich, DE*
[c] *Institut für Laser- und Plasmaphysik, Heinrich-Heine-Universität Düsseldorf, Universitätsstr. 1, D-40225 Düsseldorf, DE*
[d] *Institut für Kernphysik, Technische Universität Darmstadt, Schloßgartenstr. 9, D-64289 Darmstadt, DE*
[e] *FLA Linear Accelerator Technologies, Deutsches Elektronen-Synchrotron DESY, Notkestrasse 85, D-22607 Hamburg, DE*
[f] *Institute for Advanced Simulation, Jülich Supercomputing Centre, Forschungszentrum Jülich GmbH, D-52425 Jülich, DE*
[g] *JARA-FAME (Forces and Matter Experiments), FZJ and RWTH Aachen University, DE*
[h] *III. Physikalisches Institut B, RWTH Aachen University, D-52056 Aachen, DE*
***e-mail list**:*
i.engin@fz-juelich.de — m.buescher@fz-juelich.de — o.deppert@gsi.de — laura.di.lucchio@desy.de — r.w.engels@fz-juelich.de — s.frydrych@gsi.de — p.gibbon@fz-juelich.de — a.kleinschmidt@gsi.de — a.lehrach@fz-juelich.de — markus.roth@physik.tu-darmstadt.de — f.schlueter@fz-juelich.de — k.strathmann@fz-juelich.de — f.wagner@gsi.de

ABSTRACT: In order to investigate the polarization degree of laser-accelerated ^{3}He ions from a pre-polarized ^{3}He gas–jet target, several challenges have to be overcome beforehand. One of these includes the demonstration of the feasibility of laser-induced ion acceleration out of gas–jet targets. In particular, the ion–emission angles as well as the ion–energy spectra have to be determined for future polarization measurements. Such an experiment was performed at the PHELIX Petawatt Laser Facility, GSI Darmstadt. As laser target, both ^{4}He, and in a second step, unpolarized ^{3}He gas were applied.

XVIth International Workshop in Polarized Sources, Targets, and Polarimetry, PSTP2015,
14-18 September 2015,
Bochum, Germany

[*]Speaker.

PoS(PSTP2015)002

1. Introduction

Nuclear polarized ^{3}He is of particular importance for fundamental research since the spins of the two protons are oriented anti-parallel so that the nuclear spin is basically carried by the unpaired neutron. That is why polarized ^{3}He [1] can be used, for example, as an effective polarized neutron target for studying the neutron structure by scattering with polarized electrons [2]. For many experiments in nuclear and particle physics, such as experiments with stored particle beams, the use of polarized ^{3}He–ion beams would be advantageous. ^{3}He gas can be polarized for long times at standard conditions. However, building a spin-polarized ^{3}He ion source for nuclear and particle physics experiments with high degrees of polarization is extremely challenging. Until now, only a few approaches have shown promise — but not with the desired particle currents or an adequate beam polarization [3, 4, 5]. At Brookhaven National Lab's Relativistic Heavy Ion Collider (RHIC) attempts are now being made to develop a polarized ^{3}He ion–beam source [6].

Conventional accelerators reach fundamental, technological, and, as one of the most important aspects, financial limits of the achievable particle energies. Some of these limitations do not apply to laser-induced particle acceleration. During the past 50 years the achievable laser intensities have been increased continuously. Since the invention of chirped pulse amplification (CPA) in 1985 [7], the higher-and-higher intensities have opened new applications for laser–physics experiments. With a high-intensity laser pulse impinging on a suitable target, a relativistic plasma is formed out of which charged particles can be accelerated to energies of several MeV. An unsolved question in this context is the influence of the strong laser and plasma fields on the spins of the accelerated particles. Two scenarios are possible here: either the magnetic fields of the incoming laser beam or the induced plasma change the spin direction of the accelerated particles, or the spins are sufficiently robust that the short laser pulse has no effect on the spin alignment of a polarized target [8].

For the second scenario, there is no data given which would allow a scientifically proven estimation of the behavior of nuclear spins ($\omega_{\mathrm{larmor},^3\mathrm{He}} = 32.4\,\mathrm{MHz\,T^{-1}}\ B$) in magnetic laser–plasma fields ($B \sim \mathcal{O}\left(10^3 - 10^5\,\mathrm{T}\right)$, temporal continuance of $10^2 - 10^3$ fs). It has to be experimentally investigated if the polarization can be conserved inside plasma during laser–acceleration processes, which would open up the possibility of nuclear fusion with polarized fuel, in which the cross-sections for nuclear fusion reactions theoretically can be enhanced, leading to higher energy yields compared to the case of unpolarized fuel [9].

While the first scenario (polarization *creation* by laser–particle interactions) has already been investigated with conventional foil targets by spin-dependent hadronic proton scattering off silicon nuclei [8], for the second one (polarization *conservation* during laser–plasma interactions) polarized ^{3}He gas can be used as production target. The relaxation time of ^{3}He depends on several conditions, *e.g.* gas pressure or field gradients of an external magnetic holding field. During the ionization processes, also the absence of one electron in the atomic shell leads to a rapid decrease of the polarization degree: the interaction time τ_{HF} for the coupling of the nuclear spins to the spin of the remaining electron is of the order of about 100 ps (GHz energy level). Thus, a full ionization of the polarized ^{3}He has to be accomplished within a few picoseconds. This can readily be achieved with currently available laser intensities. We report here on preliminary results of a first measurement to demonstrate the general feasibility of laser-induced ion acceleration out of helium–gas jets at PHELIX, GSI Darmstadt. The experiments were conducted with both ^{4}He and unpolarized

^{3}He gas as laser target. The main ion–emission angles as well as the ion–energy spectra could be determined.

2. Ion Acceleration in underdense Plasmas

When a high-intensity laser pulse with laser frequency ω_L is focused onto a target, an energy transfer from the incident pulse to the atoms or molecules occurs (the so-called *heating* process) and a plasma is formed. The eigenfrequency of the collective electron motion against the plasma-ion background is called (electron) plasma frequency $\omega_p \propto \sqrt{n_e}$, with n_e being the electron number density. The relation between plasma and laser frequencies determines whether a laser pulse is able to propagate through plasma or not: it can propagate through the plasma until the plasma frequency becomes equal to the frequency of the electromagnetic wave. This limiting case is given for a critical plasma density $n_c \propto \omega_L^2$. Hence, depending on n_c, and therefore on the applied laser and target parameters, laser–plasma interactions generally can be categorized in *overdense* (*e.g.* for solid targets, $\omega_p > \omega_L$) and *underdense* (*e.g.* for gaseous targets, $\omega_p < \omega_L$) interactions with various absorption and charged particle–acceleration mechanisms [10, 11]. In underdense plasma targets, relativistic self-focusing and channeling can occur such that the laser pulse stays focused over several Rayleigh lengths and the energy transfer to the plasma electrons can remain for longer interaction times [12]. With today's laser intensities, only electrons can be accelerated directly by the incident laser pulse, *e.g.* by the ponderomotive force which is proportional to the negative radial gradient of the laser intensity, $\boldsymbol{F}_{pon} \propto -\nabla I_L$: electrons are irreversibly expelled from regions of higher intensity while the inert massive ions remain virtually unaffected on their original position. This ponderomotive process $-\mathscr{O}\left(v_{osc}^2\right)$ is symmetric, the resulting density channel is cylindrical. Large secondary electric fields of the order of several TV/m can be generated by this charge separation. The arising Coulomb forces and the given ponderomotive forces compete against each other until a Coulomb explosion takes place in which the remaining ions are accelerated radially outwards from the location of highest ion density [13].

The physics of this process can be simulated with the help of a particle-in-cell code. Within this study, EPOCH 2D [14] was used on the Jülich supercomputer JURECA. A 2D simulation box was filled with $50,000 \times 6,250$ grid points distributed over an area of $2,000\,\mu m$ in x times $250\,\mu m$ in y. The spatial resolution was 25 grid points per μm (grid size of 40 nm). Inside this box, a neutral ^{4}He/^{3}He gas jet was initialized which is then ionized by the simulated laser pulse (which propagates in positive x-direction, centered in y). The particle–density distribution was adapted from experimental interferometrical characterizations of the gas flow through a supersonic de Laval nozzle (nozzle throat of 0.5 mm, backing pressure of 25 bar): 6^{th}-order superGaussian particle–density profile with a maximal particle density of $n_{max}^{gas} = 0.06\,n_c$. The laser parameters were set according to the PHELIX parameters: focus intensity $I_L = 1.4 \times 10^{19}\,W\,cm^{-2}$, wavelength $\lambda_L = 1.053\,\mu m$, pulse duration $\tau_L = 0.8\,ps$, focus diameter FWHM of $25.7\,\mu m$, critical density $n_c = 10^{21}\,cm^{-3}$, leading to a normalized vector potential of $a_0 \approx 3.3$.

Figure 1 (a) illustrates the temporal evolution of the normalized electron (top) and He^{2+} ion densities (bottom) in pseudo colors for $t = 3.5\,ps$ (left column) and $t = 6.5\,ps$ (right column) after the laser pulse entered the box at the left boundary. A channel both in ion and electron density is generated around the laser–propagation axis. The simulation predicts strong self-focusing effects

followed by filamentation. For larger times, the channel widens and the sharp structures smear out due to the presence of several filaments. Approximately at the location of the gas–jet center (at $x \approx 900\,\mu\text{m}$), the laser pulse starts to disperse in the underdense plasma regions. The sheath of the channel for both particle species is characterized by an enhanced particle density. In Fig. 1 (b), the angular He^{2+} ion–energy distribution can be regarded. The number of simulated particles is indicated by pseudo colors. It becomes obvious, that in the transversal direction, *i.e.* around $\pm 90°$ with respect to the laser–propagation direction (0°), two peaks in ion energy $\mathscr{E}$ are present. This information is important for planning the corresponding laser beamtime (or to be more precise: the setup for ion diagnostics) beforehand. Although the simulation predicts a maximal ion energy of about 10 MeV at $\pm 90°$, the density of the plotted pseudo colors, *i.e.* the ion number, has to be considered as well: an experimentally detectable signal is not expected for the highest ion energies.

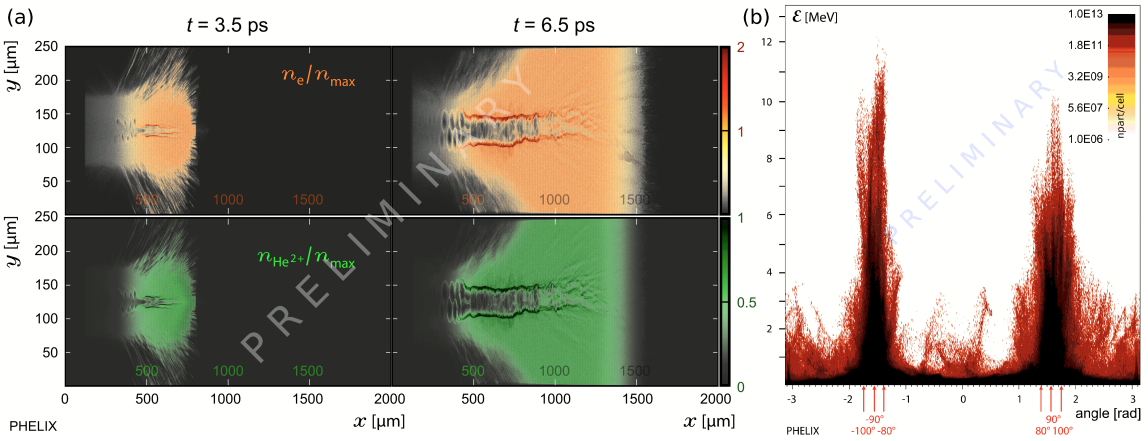

Figure 1: EPOCH-simulated data (PHELIX): (a) Temporal evolution of the normalized electron– and $^4He^{2+}$ ion–number densities for $t = 3.5\,\text{ps}$ (left column) and $t = 6.5\,\text{ps}$ after the laser pulse entered the simulation box at the left boundary. (b) Angular He^{2+} ion–energy distribution for $t = 6.5\,\text{ps}$.

3. Experimental Studies

The PHELIX parameters were set to: beam energy (after compression) of $\mathscr{E}_\text{L} = 40 - 50\,\text{J}$, pulse duration of $\tau_\text{L} = 0.4 - 1.1\,\text{ps}$, wavelength of $\lambda_\text{L} = 1.053\,\mu\text{m}$. The laser beam was focused using a 90° off-axis parabolic mirror with an f-number of 6.8. Before each shot, the elliptical laser focus was aligned to a minimal spot size ($11\,\mu\text{m} \times 15\,\mu\text{m}$). Peak intensities of about $1.4 \times 10^{19}\,\text{W cm}^{-2}$ could be reached in the focus. As laser target, both ^{4}He and unpolarized ^{3}He gas were used. A de Laval nozzle with a nozzle throat of 0.5 mm was attached in order to shape a gas jet with adequate density profile (sharp density ramps at the outer gas–jet regions with a near-flat-top profile in the center). Different backing pressures were applied during the experimental beamtime: in case of ^{4}He gas, the pressures were 30 bar and 15 bar, and in case of ^{3}He gas a maximal backing pressure of 8 bar was available. The maximal particle density inside the gas jet is proportional to the applied backing pressure in front of the nozzle: the densities for these pressure regimes in the focus height were $6 \times 10^{19}\,\text{cm}^{-3} \approx 0.06\,n_\text{c}$, $3.25 \times 10^{19}\,\text{cm}^{-3} \approx 0.03\,n_\text{c}$, and (in case of ^{3}He) $1.67 \times 10^{19}\,\text{cm}^{-3} \approx$

$0.02\,n_c$, respectively. As main ion diagnostics, a removable radiochromic film (RCF) [15] wrap-around detector was mounted close to the laser–target interaction region cylindrically around the nozzle in order to measure the angular ion distribution qualitatively. The *GAFCHROMIC HD-V2* RCFs were wrapped in 5 µm thick Al foil in order to protect the detectors from side-scattered laser light. Hence, $He^{1+,2+}$ ions with energies > 1.6 MeV were able to pierce the Al shielding and irradiate the RCF. The recorded dose on the RCF detectors was due to both ion species and gamma radiation as background signal. In addition, three Thomson parabola spectrometers (TP) [16, 17, 18] were placed at three angles relative to the laser direction (wedge-shaped capacitor with a HV of 3 kV, $B \approx 0.6$ T, covered solid angles $170 - 370$ nSr). The TPs were armed with *Agfa MD4.0* image plates (IP) [19, 20] and for one laser shot with *TASTRAK* CR-39 SSNTDs [21]. Appropriate *CST* simulations for the given TP setup were conducted in order to gain information about the energy–deflection dependencies of all ion species $\left({}^{3,4}He^{1+,2+}\right)$ inside the TP fields. Thus, experimental data for the specific deflection parameters on the IP–detector plane could directly be related to the corresponding ion energies.

Within the PHELIX experiments, ${}^{3,4}He^{1+,2+}$ ions could successfully be accelerated to MeV energies. The ion–angular distribution as well as the energy spectra for all ion species for specific emission angles could be extracted. The results are in line with the corresponding EPOCH simulations. Figure 2 illustrates the scanned image of an irradiated RCF from the left side relative to the laser–propagation direction. The gray scale values were converted in pseudo colors. In transversal direction ($\pm 90°$) a peak in ion signal with a FWHM of $\varphi_{\text{fwhm}} = 23°$ indicates the main ion–emission angles at which the TPs were aligned for the following measurements: $-\{80°, 90°, 100°\}$.

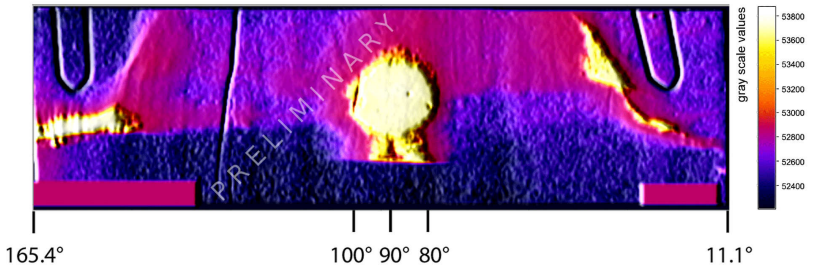

Figure 2: Irradiated RCF (left side relative to the laser–propagation direction). The FWHM of the transversal peak around $\pm 90°$ on the focus height is $\varphi_{\text{fwhm}} = 23°$.

Since the IPs used in the experiment could not be calibrated with ${}^{3,4}He^{1+,2+}$ ions beforehand, the obtained IP signals did not yield any credible quantitative information about the laser-accelerated ion number in a specific solid angle. But, the ion–energy spectra, *i.e.* the normalized signal intensity (per MeV and Sr, lin. scale) against the ion energy (in MeV, lin. scale), could be extracted from the detector raw data. In order to get an impression of the real ion number, one TP was equipped with CR-39 detectors for one laser shot. The risk of oversaturating the SSNTDs was minimized by choosing not the main ion–emission angle for the TP measurement (here: $-80°$) and by applying a decreased helium backing pressure (here: 15 bar, *i.e.* $n_{\text{max}}^{\text{gas}} = 0.03\,n_c$). Figure 3 exemplifies the laser-accelerated ion–energy spectra for one laser shot (laser energy of 43.8 J, maximal neutral He–gas density in a height of 500 µm above the nozzle exit, *i.e.* the shooting height, $n_{\text{max}}^{\text{gas}} = 0.06\,n_c$) and for the main ion–emission angle of $-90°$. Both spectra look familiar regarding

thermal energy spectra as they are common for laser-accelerated particles: a peak in ion number (or signal intensity) at low energies and a decrease in signal for higher energies with a saddle-like structure in between. $^4He^{2+}$ ions could be accelerated to higher energies, which is an important information regarding future polarization measurements of laser-accelerated $^3He^{2+}$ ions out of a polarized ^{3}He gas–jet target. Since the $^3He^{1+}$ ions are assumed to be unpolarized they will cause a disturbing background signal. In order to suppress these signals, the lower-energetic $^3He^{1+}$ ions can be filtered with Al degrader foils of adequate thickness so that a more or less pure $^3He^{2+}$ ion signal can be investigated. The high-energy and low-energy cut-offs in case of $^4He^{2+}$ in Fig. 3 are given with 4.6 MeV (with a normalized energy uncertainty of $\Delta\mathscr{E}\,\mathscr{E}^{-1} = 0.032$) and 0.84 MeV ($\Delta\mathscr{E}\,\mathscr{E}^{-1} = 0.014$). The single CR-39 measurement for extracting the real ion number for one laser shot (obtained at $-80°$, *i.e.* in a solid angle of 356 nSr, and with a smaller gas density) in total yielded approximately 1.95×10^{11} Sr^{-1} He^{1+} and He^{2+} ions. This number will be increased by choosing the main ion–emission angle for the polarimetry as well as by increasing the backing pressure to 30 bar.

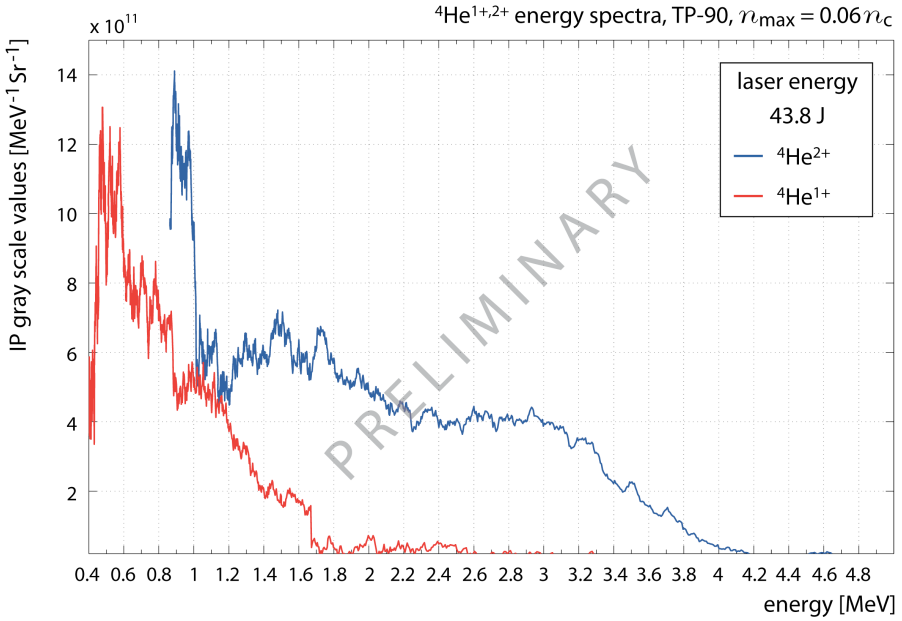

Figure 3: $^4He^{1+,2+}$ ion–energy spectra at $-90°$ relative to the laser–propagation direction: in blue $^4He^{2+}$, in red $^4He^{1+}$. Laser energy: 43.8 J. Target parameters: maximal neutral He–gas density in a height of 500 µm above the nozzle edge $n_{max}^{gas} = 0.06\,n_c$.

4. Conclusion

The experimental results proved the general feasibility of laser-driven ^{3,4}He–ion acceleration out of unpolarized gas–jet targets at PHELIX. With this *sine qua non* for a spin–polarization measurement of laser-accelerated $^3He^{2+}$ ions, an appropriate layout of a polarized ^{3}He gas–jet target available for laser–acceleration experiments can be prepared. The optimal laser and target parameters could be identified for a future laser beamtime at PHELIX.

5. Acknowledgments

The authors gratefully acknowledge the strong personal support of both R. Maier (IKP, FZ Jülich) and T. Stöhlker (HI Jena, GSI Darmstadt). Furthermore, sincere appreciation is expressed to the Institute for Nuclear Physics (IKP, FZJ) and to the Plasma Physics staff (PHELIX, GSI Darmstadt) for their great assistance. Last but not least, the authors show their gratitude to the Central Institute for Engineering, Electronics and Analytics (ZEA, FZJ) for the technical support as well as to the Institute for Laser and Plasma Physics (ILPP, HHU Düsseldorf) staff for fruitful discussions and for using their scanner.

References

[1] K. Krimmer *et al.*, *Nucl. Instr. Meth.*, vol. 611, issue 1, 2009, doi:10.1016/j.nima.2009.09.064
[2] M. Tanaka, *Nucl. Instr. Meth.*, vol. 402, no. 2-3, 1998, doi:10.1016/S0168-9002(97)00896-6
[3] D. O. Findley *et al.*, *Nucl. Instr. Meth.*, vol. 71, no. 2, 1969, doi:10.1016/0029-554X(69)90001-9
[4] W. E. Burcham *et al.*, *Nucl. Instr. Meth.*, vol. 116, no. 1, 1974, doi:10.1016/0029-554X(74)90569-2
[5] R. J. Slobodrian, *Nucl. Instr. Meth.*, vol. 185, no. 1-3, 1981, doi:10.1016/0029-554X(81)91257-X
[6] J. Maxwell *et al.*, *Phys. Part. Nuclei*, vol. 45, no. 1, 2014, doi:10.1134/S1063779614010651
[7] D. Strickland, and G. Mourou, *Opt. Commun.*, vol. 56, no. 3, 1985, doi:10.1016/0030-4018(85)90120-8
[8] N. Raab *et al.*, *Phys. Plasmas*, vol. 21, no. 2, 2014, doi:10.1063/1.4865096
[9] H. Paetz gen. Schieck, *Few-Body Syst.*, vol. 54, no. 12, 2013, doi:10.1007/s00601-012-0485-0
[10] V. T. Tikhonchuk, *Nucl. Instr. Meth.*, vol. 620, no. 1, 2010, doi:10.1016/j.nima.2010.01.051
[11] H. Daido *et al.*, *Rep. Prog. Phys.*, vol. 75, no. 5, 2012, doi:10.1088/0034-4885/75/5/056401
[12] P. Monot *et al.*, *Phys. Rev. Lett.*, vol. 74, 1995, doi:10.1103/PhysRevLett.74.2953
[13] G. S. Sarkisov *et al.*, *Phys. Rev. E*, vol. 59, 1999, doi:10.1103/PhysRevE.59.7042
[14] T. D. Arber *et al.*, *Plasma Phys. Contr. F.*, vol. 57, no. 11, 2015, doi:10.1088/0741-3335/57/11/113001
[15] W. L. McLaughlin *et al.*, *Radiat. Phys. Chem.*, vol. 10, no. 2, 1977, doi:10.1016/0146-5724(77)90017-6
[16] R. F. Schneider *et al.*, *J. Appl. Phys.*, vol. 57, no. 1, 1985, doi:10.1063/1.335389
[17] D. C. Carroll *et al.*, *Nucl. Instr. Meth.*, vol. 620, no. 1, 2010, doi:10.1016/j.nima.2010.01.054
[18] J. T. Morrison *et al.*, *Rev. Sci. Instrum.*, vol. 82, no. 3, 2011, doi:10.1063/1.3556444
[19] I. J. Paterson *et al.*, *Meas. Sci. Technol.*, vol. 19, no. 9, 2008, doi:10.1088/0957-0233/19/9/095301
[20] P. Leblans *et al.*, *Materials*, vol. 4, no. 6, 2011, doi:10.3390/ma4061034
[21] R. P. Henke *et al.*, *Nucl. Instr. Meth.*, vol. 97, no. 3, 1971, doi:10.1016/0029-554X(71)90250-3